MRO CRISM SYSTEMATIC INVESTIGATION OF THE MSL CANDIDATE LANDING SITES. F. P. Seelos[1], O. S. Barnouin-Jha[1], and S. L. Murchie[1], [1]Johns Hopkins University Applied Physics Laboratory, 11100 John Hopkins Road, MP3-E104, Laurel, MD, 20723 (Frank.Seelos@jhuapl.edu).

Introduction: In support of the ongoing Mars Science Laboratory (MSL) landing site selection process, a series of standardized Compact Reconnaissance Imaging Spectrometer for Mars (CRISM) data products were assembled for each of the ~50 candidate landing sites under consideration at the 2nd MSL landing site selection workshop. Similar systematic CRISM product sets will be prepared for future MSL workshops, with the complexity of the spectral data processing and modeling effort increasing as the number of candidate sites under consideration is reduced. The CRISM products generated in support of MSL landing site selection are available to the community at http://crism.jhuapl.edu/msl_landing_sites/.

CRISM Observing Modes and Data Processing: CRISM has two primary observing modes: multispectral push broom observations acquired at ~100 or ~200 m/pxl with 72 spectral channels, and hyperspectral gimbaled (or targeted) observations acquired at ~20 or ~40 m/pxl with 544 spectral channels. The spectral range for all CRISM observation is 0.36 to 3.92 μm [1]. CRISM observations are calibrated to radiance on sensor and I/F, and first order photometric (Lambertian) and atmospheric (empirical transmission) corrections are applied that allow observations acquired under varying geometric and atmospheric conditions to be more readily compared [2].

Summary Parameters and Browse Products. The presence and strength of spectral signatures of interest is routinely characterized by the calculation of spectral summary parameters [3]. The parameters are band math calculations designed to quantify spectral characteristics consistent with surface mineralogy or atmospheric gas absorptions. From a set of 45 routinely generated summary parameters, 7 standard RGB composites or browse products have been defined. Each is composed of a related suite of parameters with uniform stretches. For example, the phyllosilicate mineralogy browse product (PHY) is comprised of R: 2300 nm spectral drop off (indicative of Fe/Mg-bearing phyllosilicates); G: 2210 nm band depth (consistent with Al-bearing phyllosilicates or Si-OH-bearing phases); B: 1900 nm band depth (attributed to H_2O in the mineral structure). Composites that highlight mafic mineralogy (MAF), ferric and ferrous iron mineralogy (FEM), and sulfate and hydrated mineralogy (HYD) are also generated. Additional CRISM browse products include a visible color composite (RGB), the apparent reflectance at 1300 nm as a proxy for infrared albedo (IRA), and a composite tuned to H_2O or CO_2 frost or ice (ICE). Browse products assembled for the candidate MSL landing sites are derived from both regional multispectral mapping mosaics and individual hyperspectral Full Resolution Targeted (FRT, ~20 m/pixel) observations.

Overview of Candidate Landing Sites: After down-selection, six candidate landing sites are currently under consideration by the MSL project [4]: Nili Fossae Trough (Fig. 1) [5,6], Mawrth Vallis (Fig. 2) [7,8], Miyamoto Crater (Fig. 3) [9], Holden Crater Fan (Fig. 4) [10], Eberswalde Crater, and North Meridiani. The first four sites were selected based in part on the detection of phyllosilicate mineralogy. In Figs. 1-4, the first and second panels show the presence and strengths of phyllosilicate-related absorptions at these four sites at a regional scale at ~200 m/pixel, and locally near the landing site at ~20 m/pixel. In the right panels, the ~20 m/pixel IRA image near the target site is shown for reference. The 2300-nm absorption attributable to Fe/Mg-bearing phyllosilicates (red channel) is particularly strong at the Nili Fossae Trough and Mawrth Vallis sites, suggesting relatively higher phyllosilicate abundance at the optical surfaces, greater sub-pixel areal coverage, and/or less obscuration by dust and coatings. It is weaker but still easily identified at the Miyamoto Crater site, and not discernable with the standard browse product parameter stretch (though it is present) at the Holden Crater Fan site. Among the fan and deltaic deposits included in the original ~50 candidate sites, only Terby Crater exhibits a Fe/Mg phyllosilicate spectral signature in discrete layers that is comparable in strength to that observed at Nili Fossae trough, Mawrth Vallis, and Miyamoto Crater (Fig. 5). Of the six final candidates, only Mawrth Vallis shows extensive exposures having absorptions consistent with Al-bearing phyllosilicates or Si-OH-bearing phases (green channel, Fig. 2).

The six final candidate sites also differ in the mafic mineralogy exposed in the less-altered crust. The latter four sites are dominated spectrally by dust and high-Ca pyroxene-bearing, probably basaltic rock. Nili Fossae trough and Mawrth Vallis both have more extensive exposures of rock exhibiting a strong olivine signature, but only Nili Fossae Trough has extensive exposures of low-Ca pyroxene rich material typical of older Noachian rock close to the landing site.

Conclusion: The six MSL candidate landing sites currently under consideration exhibit a wide range of spectral properties. Nili Fossae Trough and Mawrth Vallis show evidence for the greatest diversity of unaltered crustal rock and the strongest signatures of phyllosilicate.

References: [1] Murchie S. L. et al. (2007) *JGR, 112*, E05S03. [2] Murchie et al. (2007) *Nature*, *in press* [3] Pelkey S. M. et al. (2007) *JGR, 112*, E08S14. [4] Golombek, M. P. et al. (2008) *this conference*. [5] Mustard, J. F. et al. (2007) *JGR, 112*, E8S04. [6] Mustard, J. F. et al. (2008) *this conference.* [7] Loizeau, D. et al. (2007) *JGR, 112*, E08S08. [8] Noe Dobrea, E. Z. et al. (2008) *this conference*. [9] Wiseman, S. M. et al. (2008) *this conference*. [10] Grant, J. A. et al. (2008) *Geology, in press.*

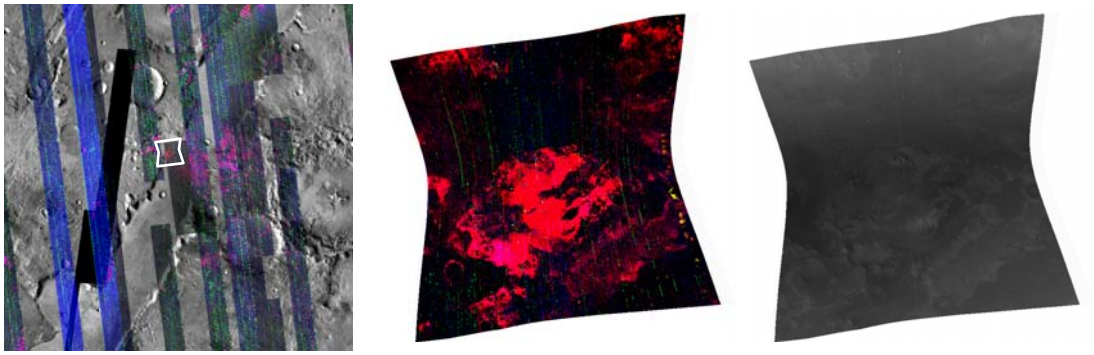

Figure 1. (left) CRISM multispectral mapping PHY browse product mosaic for the Nili Fossae Trough landing site. (center) PHY browse product derived from FRT000064D9. (right) The corresponding IRA image.

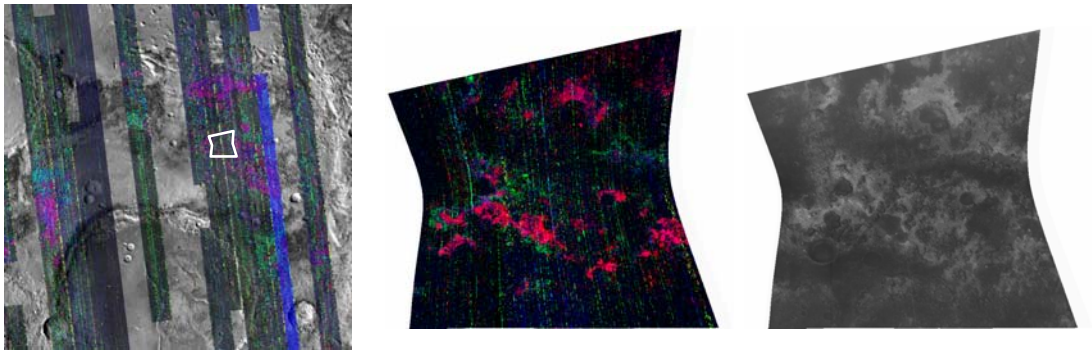

Figure 2. (left) CRISM multispectral mapping PHY browse product mosaic for the Mawrth Vallis landing site. (center) PHY browse product derived from FRT00004ECA. (right) The corresponding IRA image.

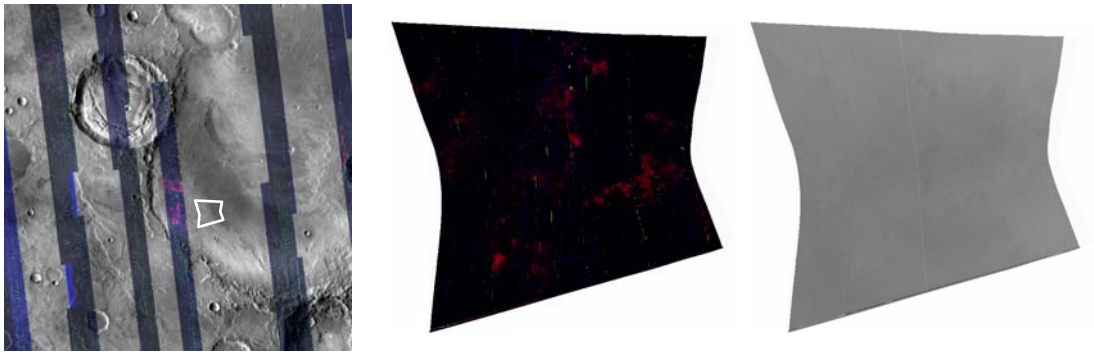

Figure 3. (left) CRISM multispectral mapping PHY browse product mosaic for the Miyamoto Crater landing site. (center) PHY browse product derived from FRT00007B8B. (right) The corresponding IRA image.

Figure 4. (left) CRISM multispectral mapping PHY browse product mosaic for the Holden Crater Fan landing site. (center) PHY browse product derived from FRT0000686C. (right) The corresponding IRA image.

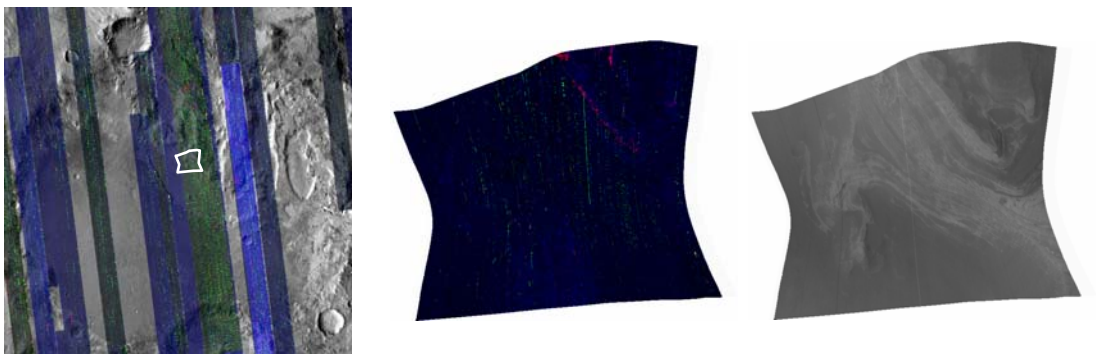

Figure 5. (left) CRISM multispectral mapping PHY browse product mosaic for the Terby Crater landing site. (center) PHY browse product derived from FRT0000622B. (right) The corresponding IRA image.